EV 10

by Diperiksa Oleh Lppm Universitas Potensi Utama

Submission date: 17-Jun-2020 04:10PM (UTC+0700)
Submission ID: 1345298150
File name: EV_10.pdf (773.28K)
Word count: 4800
Character count: 27651

March - April 2020
ISSN: 0193-4120 Page No. 7890 - 7904

Selection of Suitable Moment Invariant Features For Mycobacterium Tuberculosis Detection in Ziehl Neelsen Stained Tissue Images

Bob Subhan Riza[1], Edy Victor Haryanto S[2], Agus Harjoko[3], Sri Hartati[4], M.K. Osman[5]

[1,2]Faculty of Engineering and Computer Science, UniversitasPotensiUtama, Indonesia
[3,4] Faculty of Computer Science and Elentronics, UniversitasGadjahMada, Indonesia
[5] Faculty of Electrical Engineering, UniversitiTeknologi MARA (UiTM), Penang Campus, 13500 Permatang, PauhPulau Pinang, Malaysia

Article Info
Volume 83
Page Number: 7890 - 7904
Publication Issue:
March - April 2020

Article History
***Article Received**: 24 July 2019*
***Revised**: 12 September 2019*
***Accepted**: 15 February 2020*
***Publication**: 09 April 2020*

Abstract

Tuberculosis is a contagious disease between humans and a disease that causes death, this disease is infected by bacteria called Mycobacterium, in this paper comparing the performance of moment invariant features through region base and skeleton, the method used in this study is Hu, Zernike and Affine, and the results obtained, the best Zernike moment invariant in detection Mycobacterium Tuberculosis with above 80%.

Keywords: *Mycobacterium Tuberculosis, region base, skeleton, performance 0*

INTRODUCTION

Tuberculosis, also known as TB, is an infectious disease caused by the bacteria called Mycobacterium tuberculosis. The bacteria typically attack the lungs and referred as pulmonary TB (PTB) disease. However, it can also affect other parts of the human body such as lymph nodes, skeletal system, central nervous system, liver and pancreas, resulting in the extra-pulmonary TB (EPTB) disease.

TB is a curable disease. The disease can be cured in most people with appropriate antibiotic treatment. Unfortunately, the disease remains the second leading cause of death from an infectious disease worldwide after HIV / AIDS [1] [2]. The World Health Organization (WHO) declared TB disease as a global public health problem in 1993, as nearly 7 – 8 million cases and 1.3 – 1.6 million deaths from TB were recorded every year. In 2010, there were an estimated 8.5 – 9.2 million cases of TB and 1.2 – 1.5 million deaths worldwide [2]. In Malaysia, TB incidence showed increasing trend to 19,337 cases (67/100,000 population) in 2010, compared to the previous year [3].

Early diagnosis of TB disease is important to ensure prompt treatment and control the spread of the disease. Currently, the diagnosis of TB disease is based on finding the presence of Mycobacterium tuberculosis in a clinical specimen of sputum or organ with suspected TB. A number of methods for TB diagnosis have been developed such as chest x-ray, culture and molecular diagnosis, but the most commonly used method is through visual identification of the bacilli using a microscope [4] [5].

The difficulties in EPTB diagnosis through visual assessment of tissue sections and the rise of EPTB incidence rate has driven this research to focus on developing a computer-aided diagnosis for this disease. The main objective of this research is to

Published by: The Mattingley Publishing Co., Inc.

March - April 2020
ISSN: 0193-4120 Page No. 7890 - 7904

automate the detection of TB bacilli in tissue sections using image processing techniques and neural network. The automated detection system is based on light-microscope images, as it is the most common method for clinical diagnosis of EPTB disease.

A. Tuberculosis

Tuberculosis is an infectious disease caused by infection of a bacterium called as Mycobacterium tuberculosis (MTB) [6]. The bacterium was first discovered by Robert Koch, a German physician and scientist in 1882. It is rod-shaped with 2 – 4 m⌟ in length and 0.2 – 0.5 m⌝⌜ in width [7]. The bacterium is classified as acid-fast bacteria because it can be viewed and examined under microscope after being treated with an acid-fast staining technique. The most common acid-fast staining technique is the Ziehl-Neelsen (Z-N) method. A sample of sputum, tissue, blood, urine or bone-marrow is collected from the location of the suspected infection and stained with the Z-N stain. The staining method caused the TB bacilli stained with red colour and the background with blue colour. Figure 1 shows an example of Z-N stained tissue slide image consisting of TB bacilli. The figure illustrates numerous TB bacilli with the red colour, were scattered over the blue tissue background. A few TB bacilli were also found overlapping with each others.

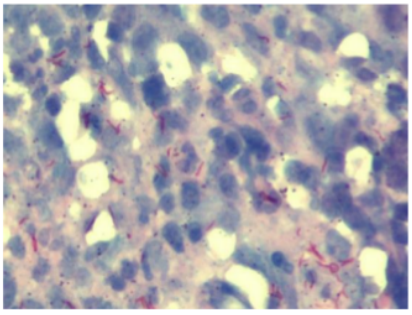

Figure 1. Z-N stained tissue slide image consisting of TB bacilli.

B. Conventional Diagnosis of Tuberculosis

TB is an infectious disease, therefore early diagnosis and treatment would not only cure the TB patient but also prevent the spreading of the disease to others. Conventional diagnosis methods can be divided into two types, latent TB infection and active TB disease.

For latent TB infection, tuberculin skin test (TST), also known as Mantoux test or purified protein derivative (PPD) test is commonly used. The test was introduced by Clement von Pirquet in 1907 [8] [9]. The purpose of TST test is to determine the presence of TB bacilli is the body. The test is conducted by injecting the PPD between the layers of the skin. The body with TB bacilli infection will distinguish the proteins of the PPD and generate an induration (bump, swelling). The induration is evaluated within 2 to 3 days after the injection by a trained medical technologist. However, the test has several disadvantages such as low sensitivity and cross react with BacilleCalmette-Guerin (BCG) vaccination as well as non-TB microbacteria, which lead to false positive result [10].

For active TB patient, conventional diagnosis includes chest X-ray, microscopic examination of clinical specimens and culture. Chest X-ray (CXR) is a non-invasive test involves acquiring a chest image by exposing the chest to radiation. The test is commonly used as suggestive of TB. It provides a rapid, cheap, convenient diagnosis and low exposure to radiation [8] [11]. However, CXR is limited for PTB diagnosis. The method also suffers limitation of low sensitivity, specificity [12] and non-specific since other illnesses can give similar features [13].

Published by: The Mattingley Publishing Co., Inc.

March - April 2020
ISSN: 0193-4120 Page No. 7890 - 7904

C. Medical Image Processing

Medical imaging is a process of acquiring images of the entire or parts of the human body for clinical application such as monitoring, inspection, diagnosis and treatment, or for medical science studies. Imaging technology for medical diagnostic purposes had started in 1895 with the discovery of x-rays. Nowadays, medical imaging has become an important part in modern medicine. The medical imaging techniques include x-ray imaging, computed-tomography (CT) imaging, magnetic resonance imaging (MRI), ultrasound imaging and visible-light imaging [14]. These techniques have been introduced to improve the quality of images and provide an accurate diagnosis.

D. Artificial Neural Networks

An artificial neural network (ANN), usually called neural network is an information processing system that is inspired by the ability of biological neural systems to process information. A neural network is composed of a large number of highly interconnected processing elements called neurons, working together to solve specific problems by using the storing experimental knowledge [15]. The past few decades have seen enormous increase of applying neural networks in a various areas such as computer science, financial, business, engineering, medicine, data mining and information systems. Medical imaging is another field for neural networks to contribute in resolving problems and providing solutions. Numerous methods have been reported in the literature applying neural networks to medical imaging such as enhancement, segmentation, compression and analysis. The following section provides a basics introduction to neural networks. Then a brief descriptions of neural network applications in medical imaging, particularly for TB detection is presented.

II. METHODS

Image Acquisition

The tissues need to be stained in order to be examined under the microscope. The staining method is called Ziehl-Neelsen (Z-N) staining method. The staining method caused the TB bacilli stained with red colour and the background with blue colour. A total of 20 Z-N stained tissue slides were used in the analysis.

Image Segmentation

Segmentation is an important step in medical image analysis. It usually serves as the basis and initial step for feature extraction, pattern recognition, image measurements and image display. Many types of segmentation techniques have been proposed in the literature for medical image analysis

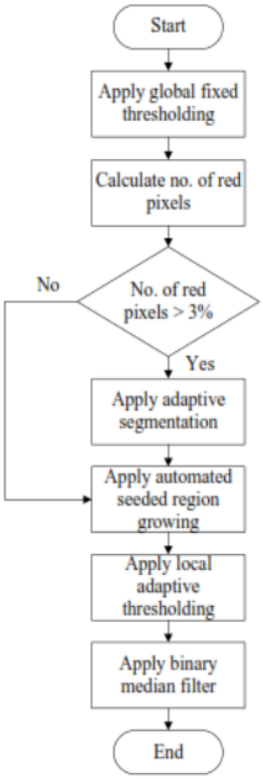

Figure 2. Flowchart of the proposed procedure for TB segmentation in tissue images

Published by: The Mattingley Publishing Co., Inc.

March - April 2020
ISSN: 0193-4120 Page No. 7890 - 7904

Segmentation techniques for sputum smears cannot be used for tissue sections due to the complexity of tissue structures and the wide range of colour spectrum that represent the TB bacilli in tissues. The only available method for detection of TB bacilli in tissue section was developed by [16]. However, Tadrous‟s method did not use any segmentation step as the detection process was achieved by generating „colour score‟ image and „shape score‟ image to calculate the probability of containing of TB bacilli in an image.

Global Fixed Thresholding

The first step of the segmentation attempted to remove non-red background pixels, as well as some red background pixels from a tissue image, so that later it will facilitate the process of TB bacilli extraction. Since the colour property is defined by hue, color segmentation can be performed based on a simple hue space. In this study, a global fixed thresholding that utilised hue component of C-Y colour model is used to remove these non-red background pixels. The method assumes the histogram of the image is bimodal, and hence the regions associated with the TB bacilli can be extracted from the background by comparing hue value of each pixel with a threshold value. Meanwhile, the saturation and luminance components are used to remove some red background pixels from the tissue image.

Feature Extraction

Feature refers to relevant information and characteristic of an object of interest. In pattern recognition, feature extraction is a process of measuring certain properties or characteristic of an object of interest that can be used to distinguish one input pattern from another pattern [17]. The purpose of feature extraction is to reduce the dimensionality of original data and improve the discriminatory information [18].

The features used in this study can be classified into three groups, simple shape descriptors, colourinformation and moment invariants. The simple shape descriptors consist of 14 features; area, perimeter, minimum and maximum radius, shape factor, dispersion, major and minor axis length, aspect ratio, ellipticity, eccentricity, tortuosity and roundness. The colour information consists of statistical properties of colour such as mean and standard deviation for an object. For the moment invariants, the three most commonly used moment invariants, Hu‟s, Zernike‟s and affine moment invariants were chosen as feature vectors. Appendix B describes the 14 simple shape descriptors, the colour information and the three moment invariants. A method for calculating these moment invariants from the skeleton of object was also proposed to improve the discrimination effectiveness. Once these features were extracted, they will be sent to the feature selection stage to determine the most discriminating features for classification.

Instead of determining moment invariants based on region information, the current study proposed a method for calculating moment invariants based on the skeleton of the object, called skeleton-based moment invariants. The method starts by applying the Zhang-Suen skeleton algorithm [19] to extract object‟s skeleton. Then the moment invariants were calculated based on the skeleton of the image. The algorithm was chosen as it provides fast processing, easy to implement and produces acceptable skeleton results for most types of digital patterns [20].

Published by: The Mattingley Publishing Co., Inc.

March - April 2020
ISSN: 0193-4120 Page No. 7890 - 7904

Table 1.List of features that have been extracted from the segmented image.

No.	Feature	No.	Feature
1	Area (A)	12	Eccentricity (ε)
2	Perimeter (P)	13	Tortuosity
3	Minimum radius (r_{min})	14	Roundness
4	Maximum radius (r_{max})	15	Mean of colour intensity
5	Shape factor (SF)	16	Standard deviation of colour intensity
6	Dispersion (D_1)	17 - 23	Region-based Hu's moment invariants ($\phi_1 - \phi_7$)
7	Dispersion (D_2)	24 - 34	Region-based Zernike's moment invariants ($S_1 - S_7$)
8	Major axis length	35 - 40	Region-based affine moment invariants ($I_1 - I_6$)
9	Minor axis length	41 - 47	Skeleton-based Hu's moment invariants ($\phi_1 - \phi_7$)
10	Aspect ratio	48 - 58	Skeleton-based Zernike's moment invariants ($S_1 - S_7$)
11	Ellipticity (E)	59 - 64	Skeleton-based affine moment invariants ($I_1 - I_6$)

New Activation Functions for HMLP Network

In general, the performance of HMLP network varies depending on the number of hidden nodes, the activation function for hidden nodes and the training algorithm. The commonly used activation function for HMLP network in literatures is sigmoid function.

Until now, there has been only one literature by Yahaya and Isa [21] that studied the performance of Elliot activation function for the HMLP network. However, the study demonstrated that sigmoid function has performed better than the Elliot function in most of the analysis. In addition, the Elliot function is rarely used and the studies related to its performance are limited.

In this paper, the hyperbolic tangent function is chosen as it is the most common choice of activation functions for MLP network [22]. The method has also demonstrated better performance than the other activation functions in several literatures [23] [24]. On top of that, two adaptive activation functions based on sigmoid and hyperbolic tangent have been proposed for the HMLP network. Detail descriptions on these activation functions along with the modifications made to adapt with the HMLP network are given in the following sub-sections.

Accuracy

For feature extraction, the present study has extracted three types of features namely simple shape descriptors, colour information and moment invariants. Simple shape descriptors consists of 14 common shape features, while two statistical parameters, mean and standard deviation of pixel intensities were used to represent colour information. Meanwhile, for the moment invariants, three region-based moments called Hu's moments, Zernike's moments and affine moment were extracted. Furthermore, a new technique for calculating moment invariants based on skeleton image was proposed to improve the robustness and accuracy of bacilli recognition. The technique adapted the Zhang-Suen algorithm to obtain the skeleton image. From the image skeleton, three moment invariants, referred as skeleton-based Hu's moments, skeleton-based Zernike's moments and skeleton-based affine moments were extracted.

III. RESULT

Analysis of Image Segmentation

The diagnosis of TB infection in tissue relies on the detection of the TB bacilli from the Z-N stained tissue slide. Colour is the most useful feature that is utilized in detecting the TB bacilli. During the staining process, carbolfuchsin dye is used to colour the TB bacilli red, while the methylene blue turns the tissues and backgrounds to the blue colour. The Z-N stain results a good contrast between the bacilli and the background, thus aiding in the detection process. However, the intensity distribution of TB bacilli and background are often varying even for the same image, as shown in Figure 3(a). The TB bacilli were found scattered through the image. Some of these bacilli appeared stained in deep red, labeled "A", while the others appeared in pale red, as indicated by "B". Moreover, under-staining and

Published by: The Mattingley Publishing Co., Inc.

March - April 2020
ISSN: 0193-4120 Page No. 7890 - 7904

over-staining issues have been frequent in tissue sections and became annoying problem in detecting the TB bacilli. Under-staining of tissue sections represents the situation of insufficient staining in which faint staining of the TB bacilli and backgrounds are observed, as shown in Figure 3(b). This situation contributes to difficulty in detecting the TB bacilli and usually leads to false negative result. In contrast, over-staining of tissue sections tends to stain red to background, resulted in false positive detection. Examples of tissue images with the over-staining problem are shown in Figure 3(c) and (d).

The proposed segmentation procedure consists of five consecutive steps which are global fixed thresholding, adaptive segmentation, ASRG, local adaptive thresholding and binary median filter. Figure 4 gives example of a tissue slide image consisting of TB bacilli and the results after applying this segmentation procedure. The first processing step involves applying the global fixed thresholding to remove non-red background pixels and some pale-red background pixels from the tissue image. Figure 4(b) depicts the result of applying the thresholding method to the original tissue image in Figure 4(a). In the paper, it was found that setting the threshold of saturation Sc-y(x-y) > 2 and luminance Yc-y(x-y) < 170 can remove these pale-red background pixels. By eliminating both non-red pixels and red background pixels significantly reduced the number of pixels that need to be processed in subsequent steps, and therefore offer faster processing speeds. As evident from Figure 4(b), the percentage of remaining pixels is 6.35% from the total number of pixels in the image.

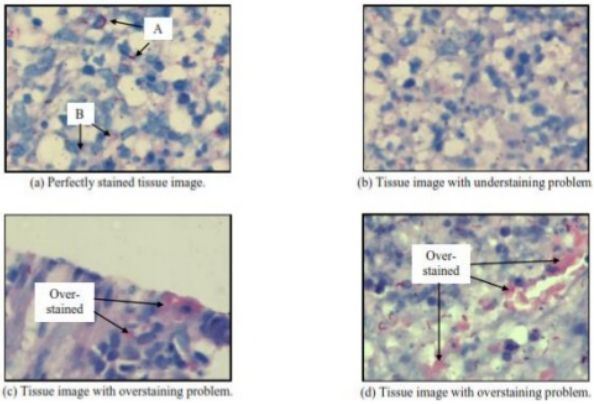

(a) Perfectly stained tissue image. (b) Tissue image with understaining problem
(c) Tissue image with overstaining problem. (d) Tissue image with overstaining problem.

Figure 3. An example of Z-N stained tissue slide image consisting of TB bacilli

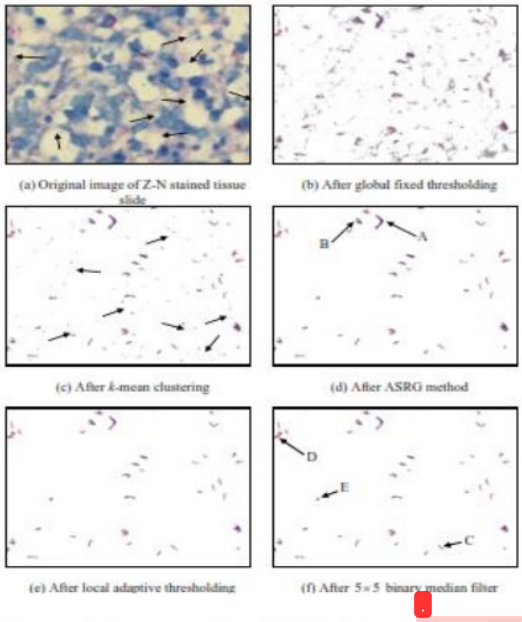

(a) Original image of Z-N stained tissue slide (b) After global fixed thresholding
(c) After *k*-mean clustering (d) After ASRG method
(e) After local adaptive thresholding (f) After 5×5 binary median filter

Figure 4. An example of Z-N stained tissue slide image and its results of applying the proposed segmentation procedure

The proposed segmentation procedure combined colour and size information for segmenting the TB bacilli. As a result, all objects that meet both specific colour and size conditions were kept while the rest were eliminated from the image. The final result of segmentation shown in Figure 4(f) contains three types of objects, single TB bacillus (labeled "C"), two or more bacilli which were partially or entirely

Published by: The Mattingley Publishing Co., Inc.

March - April 2020
ISSN: 0193-4120 Page No. 7890 - 7904

overlapped (labeled "D") and objects that do not belong to TB bacilli (labeled "E"). For the purpose of diagnosis, such unrelated objects need to be removed from the image to avoid misdiagnosis of TB. To achieve this, the subsequent step involved extracting suitable features that can be used to represent these types of objects. These features were then used to train a neural network classifier to identify those objects belong to TB bacilli and eliminate the unrelated objects.

The proposed segmentation procedure was also evaluated for tissue images with under-staining and over-staining problems. Figure 5 shows the result for tissue image with under-staining problem while Figure 6 for tissue image with over-staining problem. Several TB bacilli (arrow) were seen in pale-red colour the image with under-staining problem and in dark red for over-staining problem. The method was able to segment the TB bacilli for both images. However, the small difference of intensity between TB bacilli and background due to under-stained and over-stained problems caused a few parts of background to appear after the segmentation process. Therefore, identification and classification of TB bacilli is required after the segmentation process in order to completely remove these backgrounds. Another examples of applying the proposed segmentation.

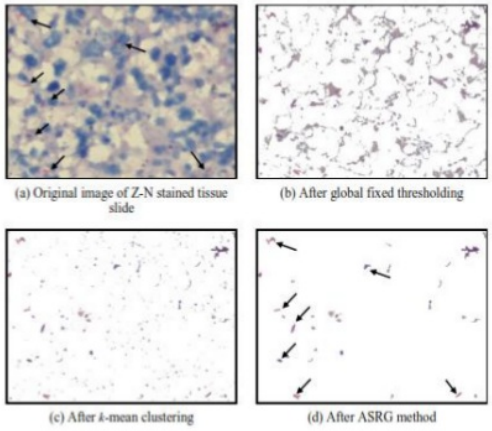

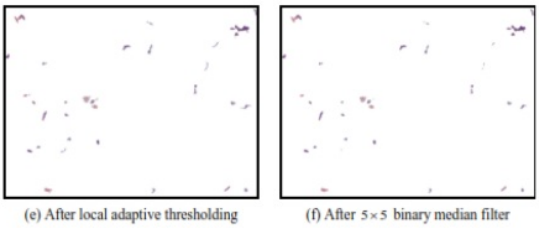

Figure 5. Results of applying the proposed segmentation procedure for tissue image with under-staining problem

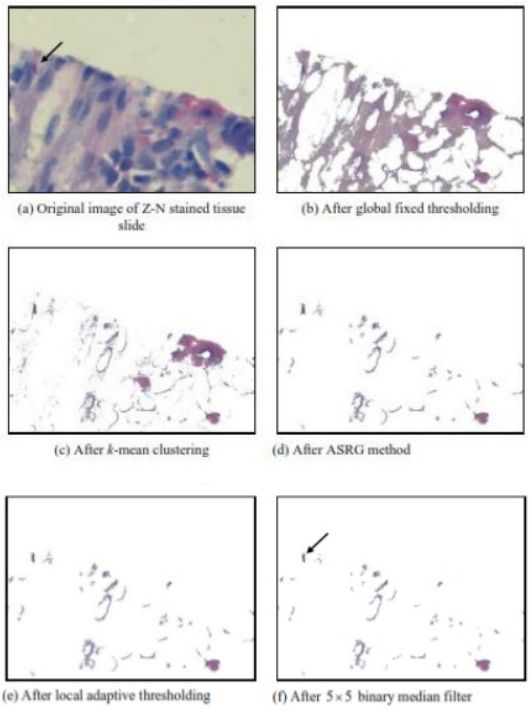

Figure 6. Results of applying the proposed segmentation procedure for tissue image with over-staining problem

Region-based Moment Invariants

The region-based moment invariants consist of three types of moments; Hu's, Zernike's and affine moment invariants. Hu's moments consist of 7 functions of moments, (ϕ_1 - ϕ_7) while the Zernike's and affine moments consist of 11, (S_1 - S_{11}) and 6 functions of moments, (I_1 – I_6), respectively. Table 2 – 4 give the classification performance as

Published by: The Mattingley Publishing Co., Inc.

measured by 5-fold cross validation using region-based Hu's, Zernike's and affine moment invariants. The average classification performance for each type of moments was further given in Table 5.

The classification results showed that the Zernike's moment invariants outperformed the Hu's and affine moment invariants significantly in representing the three types of object. Zernike's moment invariants are a type of orthogonal moment which usually has better capability in feature representation and more robust to image noise compared to the non-orthogonal moments such as Hu's and affine moment invariants [27]. In addition, Zernike's moment invariants consist more moment functions compared to the Hu's and Affine moment invariants, which allow them to provide sufficient information in representing these objects. The moments achieved the best classification accuracies of 88.71%, 88.67% and 87.13 for training, validation and testing, respectively. Conversely, Hu's and affine moment invariants were insufficient to represent the objects well. Classification accuracies using both types of moments were relatively lower compared to the Zernike's moment invariants, with all accuracies below 80.00%.

Table 2.Classification performance using region-based Hu's moment invariants.

Fold	No. of hidden nodes	No. of iteration	Accuracy (%)		
			Training	Validation	Testing
1	31	50	80.33	79.00	79.00
2	9	50	78.72	78.83	79.83
3	22	13	80.44	78.50	76.17
4	13	10	78.61	78.83	78.50
5	42	11	80.28	79.50	78.00
Average	23.4	26.8	79.68	78.93	78.30

Table 3. Classification performance using region-based Zernike's moment invariants

Fold	No. of hidden nodes	No. of iteration	Accuracy (%)		
			Training	Validation	Testing
1	35	32	89.11	89.00	87.00
2	10	50	87.89	89.17	89.00
3	22	42	89.56	89.83	85.67
4	26	33	88.83	88.50	85.83
5	12	50	88.17	86.83	88.17
Average	21.0	41.4	88.71	88.67	87.13

Published by: The Mattingley Publishing Co., Inc.

March - April 2020
ISSN: 0193-4120 Page No. 7890 - 7904

Table 4. Classification performance using region-based Affine moment invariants

Fold	No. of hidden nodes	No. of iteration	Accuracy (%)		
			Training	Validation	Testing
1	39	50	78.17	77.33	75.17
2	42	22	78.06	77.33	77.00
3	19	50	78.83	77.33	74.67
4	50	36	78.78	77.00	77.83
5	39	29	78.17	78.33	76.17
Average	37.8	37.4	78.40	77.47	76.17

Table 5. Average classification performance using various region-based moment invariants.

Types of region based moments	Average hidden nodes	Average iterations	Accuracy (%)			Average
			Training	Validation	Testing	
Hu's	23.4	26.8	79.68	78.93	78.30	78.97
Zernike's	21.0	41.4	**88.71**	**88.67**	**87.13**	**88.17**
Affine	37.8	37.4	78.40	77.47	76.17	77.34

Figure 7 shows more detailed information about the classification performance according to different types of objects using Hu's, Zernike's and affine moment invariants. The ability to recognize the type of an object differed according to the types of moment. The Hu's and Zernike's moment invariants were good in representing objects belonging to "TB" while the affine moment invariants were good for objects belonging to "overlapped TB". Overall, the Zernike's moment invariants provided the best features in representing all types of objects, with the highest percentage of accuracies for training, validation and testing.

Skeleton-based Moment Invariants

In this paper, skeleton-based moment invariants were introduced to improve the classification of segmented objects. To obtain these features, the Zhang-Suen skeleton algorithm was applied to the segmented objects to produce image skeletons. Figure 8 shows examples of tissue images after applying image segmentation and their skeleton image. Then, the Hu's, Zernike's and affine moment invariants of each object were calculated from the object's skeleton. These moments were further called as skeleton-based Hu's moment invariants, skeleton-based Zernike's moment invariants and skeleton-based affine moment invariants. Table 6 - 8 give the classification performance for skeleton-based Hu's, Zernike's and affine moment invariants as evaluated using a 5-fold cross validation technique. Then, their performances were averaged and presented in Table 9.

Published by: The Mattingley Publishing Co., Inc.

March - April 2020
ISSN: 0193-4120 Page No. 7890 - 7904

Table 6.Classification performance using skeleton-based Hu's moment invariants.

Fold	No. of hidden nodes	No. of iteration	Accuracy (%)		
			Training	Validation	Testing
1	14	50	80.44	79.83	78.83
2	3	50	80.06	80.33	80.83
3	7	50	80.67	80.17	78.67
4	32	50	82.11	79.83	79.17
5	10	41	80.22	79.83	79.67
Average	13.2	48.2	80.70	80.00	79.43

Table 7.Classification performance using skeleton-based Zernike's moment invariants.

Fold	No. of hidden nodes	No. of iteration	Accuracy (%)		
			Training	Validation	Testing
1	20	50	88.78	88.00	88.83
2	13	50	88.11	88.83	88.50
3	27	40	90.06	88.83	86.00
4	15	48	89.39	88.17	85.67
5	21	50	89.44	87.00	87.17
Average	19.2	47.6	89.16	88.17	87.23

Table 8. Classification performance using skeleton-based Affine moment invariants.

Fold	No. of hidden nodes	No. of iteration	Accuracy (%)		
			Training	Validation	Testing
1	26	50	79.33	80.17	79.50
2	30	50	80.94	81.17	80.50
3	37	44	81.17	80.83	76.67
4	28	39	80.94	80.83	78.00
5	41	34	81.06	80.17	78.00
Average	32.4	43.4	80.69	80.63	78.53

Published by: The Mattingley Publishing Co., Inc.

March - April 2020
ISSN: 0193-4120 Page No. 7890 - 7904

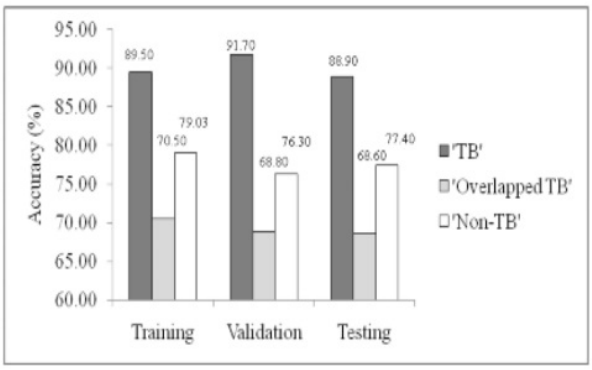

(a) Region-based Hu's moment invariants

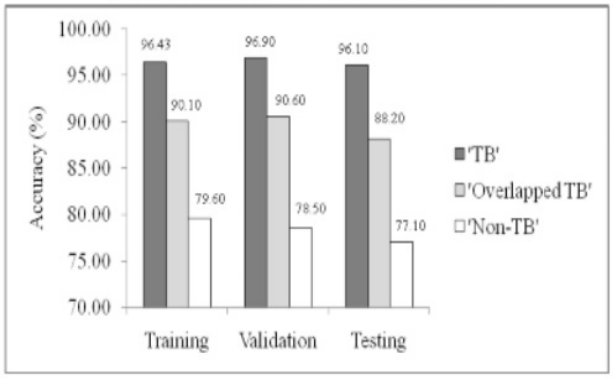

(b) Region-based Zernike's moment invariants

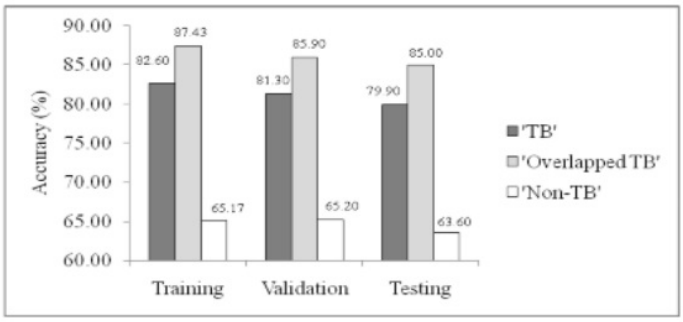

(c) Region-based affine moment invariants

Figure 7.Classification performance according to the types of object using region-based Hu's, Zernike"' and affine moment invariants.

Published by: The Mattingley Publishing Co., Inc.

March - April 2020
ISSN: 0193-4120 Page No. 7890 - 7904

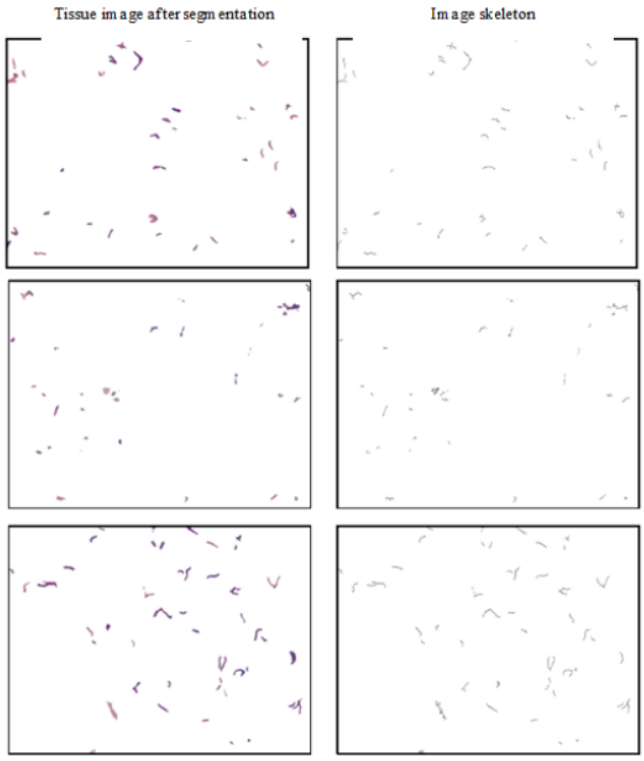

Figure 8.Examples of tissue images after image segmentation and their skeleton images.

Table 3. Average classification performance using various skeleton-based moment invariants.

Types of skeleton- based moments	Average hidden nodes	Average iterations	Accuracy (%)			Average
			Training	Validation	Testing	
Hu's	13.2	48.2	80.70	80.00	79.43	80.04
Zernike's	**19.2**	**47.6**	**89.16**	**88.17**	**87.23**	**88.19**
Affine	32.4	43.4	80.69	80.63	78.53	79.95

The skeleton-based Zernike's moment invariants were found to be the best features among all skeleton-based moment invariants. The moments achieved the highest classification performance for training, validation and testing with accuracies of 89.16%, 88.17% and 87.23%, respectively. Meanwhile, the lowest classification performance was achieved by using the skeleton-based affine moment invariants. The moments achieved the lowest training and testing accuracies of 80.69% and 78.53%, respectively.

Classification of objects in tissue images has been improved by applying the skeleton algorithm before calculating moment invariants. By introducing skeleton method has reduced an object to its essential structure, and therefore provided better representation for the object. It was demonstrated

Published by: The Mattingley Publishing Co., Inc.

March - April 2020
ISSN: 0193-4120 Page No. 7890 - 7904

that for each type of moments, a slight increase in classification accuracy (0.10% □ 3.16%) was recorded during the training, validation and testing, except for the validation accuracy of Zernike's moments.

Both "overlapped TB" and "non-TB" objects usually appear in various shapes and sizes which make them difficult for classification. However, the skeleton-based moment invariants provided better representation for both types of objects. Figure 9 gives the detailed classification performance according to different types of objects using Hu's, Zernike's and affine moment invariants. It can be seen that classification performance of both "non-TB" objects seems to improve significantly using the skeleton-based moment invariants, while there were slight improvements for the "overlapped-TB" by using this method. However, the method has also resulted in slight performance degradation in classifying objects belong to "TB". Overall, the skeleton-based Zernike's moment invariants provided the best results, with the highest classification accuracies on training and testing, where other moment invariants showed marginally better success.

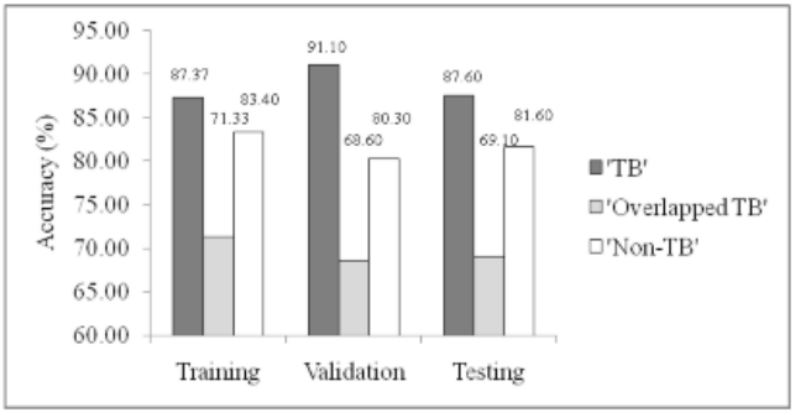

(a) Skeleton-based Hu's moment invariants.

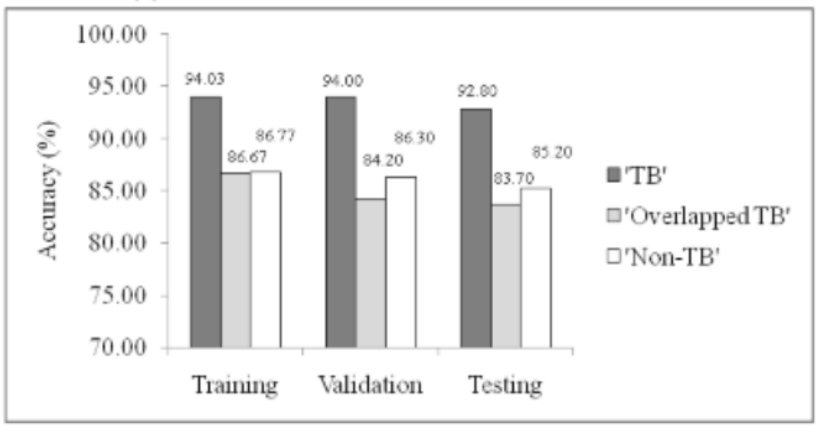

(b) Skeleton-based Zernike's moment invariants.

Published by: The Mattingley Publishing Co., Inc.

March - April 2020
ISSN: 0193-4120 Page No. 7890 - 7904

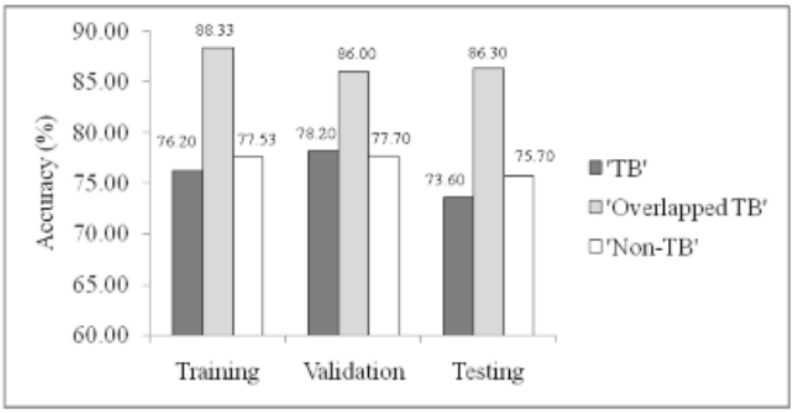

(c) Skeleton-based affine moment invariants

Figure 9.Classification performance according to the types of object using skeleton-based Hu's, Zernike's and Affine moment invariants.

IV. CONCLUSION

Result of this research is Zernike's moment is the best moments invariant for detection of Mycobacterium Tuberculosis

ANNOUNCEMENT

The author thanks the Directorate General of Research and Development Strengthening DRPM for funding this research and also to the UniversitasPotensiUtama for providing support and attention to this research.

REFERENCES

[1] Freiden, T.R., Sterling, T.R., Munsiff, S.S., Watt, C.J., & Dye, C. (2003). Tuberculosis. Lancet, 362, 887-899.

[2] WHO. (2011). Global Tuberculosis Control 2011: World Health Organization (WHO).

[3] MAPTB. (2012). MAPTB Newsletter. Kuala Lumpur : Malaysian Association for the Prevention of Tuberculosis (MAPTB).

[4] Khatun, Z., Hossain, MS, Roy, CK, Sultana, T., Rahman, MQ, Azad, M.B.A.S. (2011). Light Emitting Diode (LED) Fluorescent Microscopy: a Milestone in the Detection of Paucibacillary Mycobacterium in Case of Pulmonary Tuberculosis. Bangladesh Medical Journal, 40(1), 22-26.

[5] Sreeramareddy, C., Panduru, K., Menten, J., & den Ende, J.V. (2009). Time Delays in Diagnosis of Pulmonary Tuberculosis: A Systematic Review of Literature. BMC Infectious Diseases, 9(1), 91.

[6] Solovic, I, Jonsson, J, Korzeniewska-Kosela, M, Chiotan, DI, Pace-Asciak, A, Slump, E. (2013). Challenges in Diagnosing Extrapulmonary Tuberculosis in the European Union, 2011.EuroSurveillance, 18(12), 1-9.

[7] Todar, Kenneth. (2012). Todar's Online Textbook of Bacteriology. Retrieved 9th February 2012, from http://textbookofbacteriology.net/tuberculosis.html.

[8] Lagne, C., & Mori, T. (2010). Advances in the Diagnosis of Tuberculosis. Respirology,15(2), 220-240.

[9] Shashidhara, A.N., &Chaudhuri, K. (1990). The Tuberculin Skin Test: Emerging 100 Years Since Its First Use. National Tuberculosis Institute Newsletter, 26(1 & 2), 116.

[10] Lee, J.Y., Choi, H.J., Park, I.N., Hong, S.B., Oh, Y.M., Lim, C.M. (2006). Comparison of Two Commercial Interferon-γ Assays for Diagnosing Mycobacterium tuberculosis Infection. European Respiratory Journal, 28(1), 24-30.

Published by: The Mattingley Publishing Co., Inc.

March - April 2020
ISSN: 0193-4120 Page No. 7890 - 7904

[11] Wood, R. (2009). Challenges of TB Diagnosis and Treatment in South Africa. Southern African Journal of HIV Medicine, 8(2), 44-48.

[12] Al Zahrani, K., Al Jahdali, H., Poirier, L., Rene, P., Gennaro, ML, &Menzies, D. (2000).Accuracy and Utility of Commercially Available Amplification and Serologic Tests for the Diagnosis of Minimal Pulmonary Tuberculosis. American Journal of Respiratory and Critical Care Medicine, 162(4), 1323.

[13] OxfordImmunotec. (2010). Tuberculosis.Retrieved 29th February, 2012, from http://www.oxfordimmunotec.com/Tuberculosis_International.

[14] Haidekker, M.A. (2011). Advanced Biomedical Image Analysis. New Jersey: Wiley Online Library.

[15] Haykin, S. (1999). Neural Networks: A Comprehensive Foundation. Englewood Cliffs, NJ:Prentice Hall.

[16] Tadrous, P.J. (2010). Computer-Assisted Screening of Ziehl-Neelsen-Stained Tissue for Mycobacteria Algorithm Design and Preliminary Studies on 2,000 Images. American Journal of Clinical Pathology, 133(6), 849-858.

[17] Rathi, V.P.G.P., &Palani, S. (2012). A Novel Approach for Feature Extraction and Selection on MRI Images for Brain Tumor Classification. Computer Science & Information Technology 225–234.

[18] Haifeng, L., Tao, J., &Keshu, Z. (2006). Efficient and robust feature extraction by maximum margin criterion.Neural Networks, IEEE Transactions on, 17(1), 157165. doi:10.1109/tnn.2005.860852.

[19] Zhang, T.S., &Suen, C.Y. (1984). A Fast Parallel Algorithm for Thinning Digital Patterns. Communications of the ACM, 27(3), 236-239.

[20] Widiarti, A.R. (2011). Comparing Hilditch, Rosenfeld, Zhang-Suen, and Nagendraprasad-Wang-Gupta Thinning. World Academy of Science, Engineering and Technology, 78, 150.

[21] Yahaya, S.Z., & Mat-Isa, N.A.M. (2011, 4-6 March). Implementation of HMLP Network with Different Activation Function for Cervical Cells Classification. Paper presented at the 7th International Colloq. on Signal Processing and its Applications (CSPA 2011), Penang, Malaysia.

[22] Karlik, B., &Olgac, A. V. (2010). Performance Analysis of Various Activation Functions in Generalized MLP Architectures of Neural Networks. International Journal of Artificial Intelligence and Expert Systems, 1(4), 111-122.

[23] Ozkan, C., &Erbek, F.S. (2003). A Comparison of Activation Functions for Multispectral Landsat TM Image Classification. Photogrammetric Engineering and Remote Sensing, 69(11), 1225-1234.

[24] Tong, D.L., &Mintram, R. (2010). Genetic Algorithm-Neural Network (GANN) : A Study of Neural Network Activation Functions and Depth of Genetic Algorithm Search Applied to Feature Selection. International Journal of Machine Learning and Cybernetics, 1(1), 75-87.

[25] Mashor, M.Y. (2009). On-Line Nonlinear Modelling and Forecasting Of Streamflow Using Neural Network. International Journal of The Computer, the Internet and Management, 17(1), 44-54.

[26] M. K. Osman, M. Y. Mashor and H. Jaafar, "Online sequential extreme learning machine for classification of mycobacterium tuberculosis in ziehl-neelsen stained tissue," 2012 International Conference on Biomedical Engineering (ICoBE), Penang, 2012, pp. 139-143.

[27] Mukundan, R. (2004). Some computational aspects of discrete orthonormal moments.Image Processing, IEEE Transactions on, 13(8), 1055-1059. doi:10.1109/tip.2004.828430

Published by: The Mattingley Publishing Co., Inc.

EV 10

ORIGINALITY REPORT

11%	7%	2%	7%
SIMILARITY INDEX	INTERNET SOURCES	PUBLICATIONS	STUDENT PAPERS

MATCH ALL SOURCES (ONLY SELECTED SOURCE PRINTED)

4%

★ ajbasweb.com

Internet Source

Exclude quotes	Off	Exclude matches	< 2%
Exclude bibliography	Off		